Chapter 5

Electromagnetic Scattering

In this chapter, we will apply the methods discussed in the preceding chapters to compute cross sections of some simple electromagnetic processes involving charged leptons (and photons, of course). We will restrict ourselves to initial and final states involving no more than two particles, and to the lowest order in perturbative calculations, (i.e., to tree-level Feynman diagrams only). The coupling at each vertex is proportional to the electric charge e of the fermion (we will only deal with charged leptons in this chapter). At low energies, this is manifested in terms of the fine structure constant

$$\alpha = \frac{e^2}{4\pi} = \frac{1}{137}. \tag{5.1}$$

The value of α depends on the energy at which it is measured. The above value corresponds to the $E \to m_\ell$ limit. Moreover, up to energies a few GeV below M_W (=80 GeV) weak interactions can be safely ignored. Strong interactions are irrelevant in this context since leptons carry no color charge. Each higher order diagram will make a contribution proportional to α to the matrix element, which will subsequently have to be squared to get the cross section. Since leading-order diagrams for $2 \to 2$ processes involve 2 vertices, our calculations will actually hold good to a few parts per 10^{-4} level at low energies.

Before looking at some examples of electromagnetic scattering between two fermions, let us recall the conserved current density in Eq. 3.33. Putting in the (free) fermion wave functions given by Eq. 3.43 in the initial and final states, we see that the *transition current* at each vertex is

$$J^\mu_{fi} = -e\bar{\psi}_f \gamma^\mu \psi_i = -e\bar{u}_f \gamma^\mu u_i \exp\left(i(p_f - p_i)\cdot x\right), \tag{5.2}$$

where u_i and $\bar{u}_f$ are the fermion spinors in the initial and final states, respectively. Such a factor at each end of a photon propagator is exactly what one would get by following the Feynman rules summarized in the last chapter.

It is instructive to note that if we had a scalar (i.e. spin-0) charged particle instead of the spin-$\frac{1}{2}$ fermion, then the transition current could be obtained by simply dropping the spinors and the γ^μ from Eq. 5.2, while retaining the normalization:

$$J^\mu_{fi} = -e(p_f + p_i)^\mu \exp\left(i(p_f - p_i)\cdot x\right). \tag{5.3}$$

Operating on the electromagnetic vector field A^μ, such a current would give the interaction only of the electric charge and the photon. The difference between the two transition currents is due to the magnetic moment of the fermion. Indeed, the lepton-photon interaction at a vertex can be expressed in the form

$$\bar{u}_f \gamma^\mu u_i = \frac{1}{2m}\bar{u}_f((p_f + p_i)^\mu + i\sigma^{\mu\nu}(p_f - p_i)_\nu)u_i, \tag{5.4}$$

known as the *Gordon decomposition* (into charge and magnetic moment parts).

5.1 Electron-Muon Scattering

Consider the process $e^-\mu^- \to e^-\mu^-$ shown in Fig. 5.1.

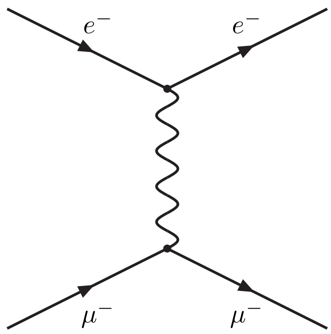

Figure 5.1: The Feynman diagram for $e^-\mu^- \to e^-\mu^-$.

The matrix element representing the exchange of a single photon between the electron and the muon currents is given, as prescribed by the Feynman rules, by

$$\mathcal{M}_{fi} = -J^\alpha_{e^-}\frac{g_{\alpha\beta}}{q^2 + i\varepsilon}J^\beta_{\mu^-} = -e^2\frac{\bar{u}(p_f^{e^-})\gamma^\alpha u(p_i^{e^-})\bar{u}(p_f^{\mu^-})\gamma_\alpha u(p_i^{\mu^-})}{q^2 + i\varepsilon}, \tag{5.5}$$

where the photon momentum q^μ is determined by the momentum conservation condition

$$q = p_i^{e^-} - p_f^{e^-} = p_f^{\mu^-} - p_i^{\mu^-}. \tag{5.6}$$

Note that switching the e^- and the μ^- in the above expression is of no consequence since the direction of the photon-mediated momentum transfer is irrelevant and will have to be integrated over to get the cross section anyway.

For the cross section, we'll need $|\mathcal{M}_{fi}|^2$, which can be written as

$$|\mathcal{M}_{fi}|^2 = \frac{e^4}{q^4}(L_{e^-})^{\alpha\beta}(L_{\mu^-})_{\alpha\beta} \tag{5.7}$$

in terms of the tensors

$$(L_{\ell^-})_{\alpha\beta} \equiv \frac{1}{e^2}(J_{\ell^-})_\alpha (J_{\ell^-})^*_\beta. \tag{5.8}$$

Evaluation of these tensors are actually much easier than it may appear at this point. A general method exists to facilitate such calculations, and it does not depend on any specific representation of the γ matrices or spinors.

Our task is to evaluate the matrix element $\bar{u}(p_2)O_\alpha u(p_1)$, where O_α is a 4×4 matrix, made of momenta and γ matrices, in the spinor space. Here α represents a collection of Lorentz indices: no index represents a scalar, one a vector, and so on. Squaring the matrix element we get a tensor, such as those in Eq. 5.8, which will make up a part of $|\mathcal{M}_{fi}|^2$, as in Eq. 5.7. Since the complex conjugate and Hermitian conjugate are the same for a complex number, the tensor is

$$\begin{aligned}(\bar{u}(p_2)O_\alpha u(p_1))(\bar{u}(p_2)O_\beta u(p_1))^* &= (\bar{u}(p_2)O_\alpha u(p_1))(u^\dagger(p_1)O_\beta^\dagger \gamma_0 u(p_2)) \\ &= (\bar{u}(p_2)O_\alpha u(p_1))(\bar{u}(p_1)\gamma_0 O_\beta^\dagger \gamma_0 u(p_2)).\end{aligned} \tag{5.9}$$

We define $\bar{O}_\beta \equiv \gamma_0 O^\dagger \gamma_0$.[1] Then, expressing the matrix multiplications in terms of the element indices, we get

$$\begin{aligned}&(\bar{u}(p_2)O_\alpha u(p_1))(\bar{u}(p_2)O_\beta u(p_1))^* \\ &\quad = \bar{u}(p_2)_i (O_\alpha)_{ij} u(p_1)_j)(\bar{u}(p_1)_k (\bar{O}_\beta)_{kl}\gamma_0 u(p_2))_l \\ &\quad = (u(p_2)_l \bar{u}(p_2)_i)(O_\alpha)_{ij}(u(p_1)_j \bar{u}(p_1)_k)(\bar{O}_\beta)_{kl}\end{aligned} \tag{5.10}$$

[2] If we define a matrix whose m, n component is $u(p_1)_m \bar{u}(p_1)_n$, the above expression is just the trace of a matrix that is the product of 4 matrices. Thus, we can write the squared matrix element of Eq. 5.9, without explicit use of the indices, as

$$(\bar{u}(p_2)O_\alpha u(p_1))(\bar{u}(p_2)O_\beta u(p_1))^* = \mathrm{Tr}(u(p_2)\bar{u}(p_2)O_\alpha u(p_1)\bar{u}(p_1)\bar{O}_\beta). \tag{5.11}$$

So, with simple expressions for the 4×4 matrix $u(p)\bar{u}(p)$, our calculations are reduced to taking traces using the relations listed in Sec. 3.2.

Now we are ready to handle the summing of spinors in the initial and final states. Commonly, the incoming beams are unpolarized and the spin polarization of the outgoing particles are undetermined. In such a case, we must take

[1] For $O_\beta = \gamma_\mu, \gamma_\mu\gamma_5, i\gamma_5, \sigma_{\mu\nu}$, $\bar{O}_\beta = O_\beta$.

[2] Einstein summation is implied, but the Latin indices label the components of the 4-component Dirac spinor, and hence run from 1 to 4. They have nothing to do with the components of a Lorentz 4-vector in the Minkowski space. X^i and X_i are one and the same.

the average of the helicities in the initial state and sum over those in the final state, which appear only in the 4×4 matrices constructed from the spinors. The matrices O_α, $\bar{O}_\beta$ do not depend on helicity. The sums can be derived from the spinors in Eq. 3.48, which simply yield

$$\sum_{\lambda=1,2} u(p,\lambda)\bar{u}(p,\lambda) = \not{p} + m \tag{5.12}$$

for fermions, and

$$\sum_{\lambda=1,2} v(p,\lambda)\bar{v}(p,\lambda) = \not{p} - m \tag{5.13}$$

for antifermions, where the helicity λ is now indicated explicitly in the spinor. Thus, after summing over the helicities of all the spin-$\frac{1}{2}$ particles in Eq. 5.11, we get

$$(\bar{u}(p_2)O_\alpha u(p_1))(\bar{u}(p_2)O_\beta u(p_1))^* = \mathrm{Tr}((\not{p}_2 + m_2)O_\alpha(\not{p}_1 + m_1)). \tag{5.14}$$

For each antiparticle, each $\not{p}+m$ is replaced by $\not{p}-m$. These expressions appear repeatedly in calculations involving spin-$\frac{1}{2}$ particles in the initial and final states of a process. They embody the linearity requirement of quantum mechanics, where $\mathcal{M}_{fi}$ must contain a single power of each spinor leading to a product of the form $u(p)\bar{u}(p)$ in the square of the matrix element.

If the helicity of a spin-$\frac{1}{2}$ particle is fixed in the initial state or determined in the final state, then the matrix element will be a function of its helicity λ. One could use explicit spinors to calculate this, but an alternative form has been derived that can be used simply in trace calculations. Consider the spin-$\frac{1}{2}$ particle in its rest frame. Define a spin 3-vector in this frame as $\vec{s} = \chi^\dagger \vec{\sigma} \chi$, where χ is normalized so that $\chi^\dagger \chi = 1$. We can construct $s^\mu = (0, \vec{s})$, which transforms as a Lorentz 4-vector. So, $p \cdot s = 0$ is a Lorentz scalar. Using the spinors in Eq. 3.48, we can show that

$$\begin{aligned} u(p,\lambda)\bar{u}(p,\lambda) &= (\not{p} + m)\frac{(1 + \gamma_5 \not{s}(\lambda))}{2} \\ v(p,\lambda)\bar{v}(p,\lambda) &= (\not{p} - m)\frac{(1 + \gamma_5 \not{s}(\lambda))}{2}. \end{aligned} \tag{5.15}$$

Defining $\hat{e}(\lambda)$ as a unit vector along $\vec{p}$ for positive helicity and opposite $\vec{p}$ for negative helicity,

$$s = \left(\frac{\hat{e}(\lambda) \cdot \vec{p}}{m}, \frac{\hat{e}(\lambda) E}{m} \right) \tag{5.16}$$

gives $s(\lambda)$ for the two helicity choices. These spin-dependent expressions become indispensable in the studies of weak interactions, where parity violation makes helicity selection a quintessential feature.

Returning to the calculation of $e^-\mu^-$ scattering cross section with unpolarized incoming beams, and no discrimination on helicities of the outgoing particles, we take the average over the initial helicities (which amounts to summing and dividing by 2) and sum over the final ones to get

$$(L_{\ell^-})_{\alpha\beta} = \frac{1}{2}\mathrm{Tr}\left((\not{p}_f^{\ell^-} + m_\ell)\gamma_\alpha(\not{p}_i^{\ell^-} + m_\ell)\gamma_\beta\right), \tag{5.17}$$

where $\ell = e, \mu$.

The expression on the RHS has two terms with an even number of γ matrices, which can be evaluated by the trace formulae of Sec. 3.2:

$$\begin{aligned}(L_{\ell^-})_{\alpha\beta} &= \tfrac{1}{2}\left(\mathrm{Tr}(\not{p}_f^{\ell^-}\gamma_\alpha\not{p}_i^{\ell^-}\gamma_\beta) + m_\ell^2\mathrm{Tr}(\gamma_\alpha\gamma_\beta)\right) \\ &= 2\left((p_f^{\ell^-})_\alpha(p_i^{\ell^-})_\beta + (p_f^{\ell^-})_\beta(p_i^{\ell^-})_\alpha - (p_f^{\ell^-}\cdot p_i^{\ell^-} - m_\ell^2)g_{\alpha\beta}\right).\end{aligned} \tag{5.18}$$

Multiplying the tensors for the electron and the muon, we get finally the unpolarized result for $|\mathcal{M}_{fi}|^2$, summed over final spins:

$$\begin{aligned}\frac{1}{4}\sum_{\text{spins}}|\mathcal{M}_{fi}|^2 &= \frac{8e^4}{q^4}((p_f^{e^-}\cdot p_f^{\mu^-})(p_i^{e^-}\cdot p_i^{\mu^-}) + (p_f^{e^-}\cdot p_i^{\mu^-})(p_i^{e^-}\cdot p_f^{\mu^-}) \\ &\quad -m_e^2(p_i^{\mu^-}\cdot p_f^{\mu^-}) - m_\mu^2(p_i^{e^-}\cdot p_f^{e^-}) + 2m_e^2m_\mu^2).\end{aligned} \tag{5.19}$$

This final result is a Lorentz invariant that is symmetric under the exchange $e^- \leftrightarrow \mu^-$.

In the extreme relativistic limit, the terms involving the particle masses can be neglected. This leads to the approximation

$$\sum_{\text{spins}}|\mathcal{M}_{fi}|^2 \approx \frac{8e^4}{(p_i^{e^-} - p_f^{e^-})^4}((p_f^{e^-}\cdot p_f^{\mu^-})(p_i^{e^-}\cdot p_i^{\mu^-}) + (p_f^{e^-}\cdot p_i^{\mu^-})(p_i^{e^-}\cdot p_f^{\mu^-})). \tag{5.20}$$

Also, in this limit, the Mandelstam variables of Eqs. 1.44, 1.45, and 1.46 become

$$\begin{aligned}s &= (p_i^{e^-} + p_i^{\mu^-})^2 = (p_f^{e^-} + p_f^{\mu^-})^2 \approx 2p_i^{e^-}\cdot p_i^{\mu^-} \approx 2p_f^{e^-}\cdot p_f^{\mu^-}, \\ t &= (p_f^{e^-} - p_i^{e^-})^2 = (p_f^{\mu^-} - p_i^{\mu^-})^2 \approx -2p_i^{e^-}\cdot p_f^{e^-} \approx -2p_i^{\mu^-}\cdot p_f^{\mu^-}, \\ u &= (p_f^{\mu^-} - p_i^{e^-})^2 = (p_f^{e^-} - p_i^{\mu^-})^2 \approx -2p_f^{\mu^-}\cdot p_i^{e^-} \approx -2p_f^{e^-}\cdot p_i^{\mu^-}.\end{aligned} \tag{5.21}$$

Thus, for scattering of unpolarized electrons and muons at $E \gg m_\mu (\approx 200m_e)$, we have a compact expression for the squared matrix element:

$$\sum_{\text{spins}}|\mathcal{M}_{fi}|^2 \approx 2e^4\frac{(s^2+u^2)}{t^2}. \tag{5.22}$$

Note that this diverges in the limit of $t \to 0$ (no momentum transfer).

What remains in the calculation of the cross section is the integration over the phase space. For final states consisting of any two given particles, the only spatial variable is the scattering angle (evaluated in the center of mass, unless otherwise specified.) The differential cross section is obtained by substituting the above $|\mathcal{M}_{fi}|^2$ in Eq. 4.21.

5.2 e^+e^- annihilation to $\mu^+\mu^-$

The Feynman diagram for the process $e^+e^- \to \mu^+\mu^-$ is shown in Fig. 5.2.

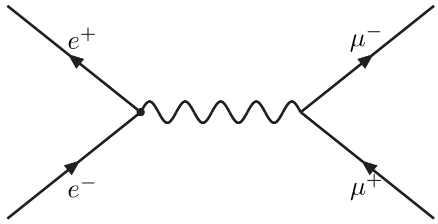

Figure 5.2: The Feynman diagram for $e^+e- \to \mu^+\mu^-$.

The squared matrix element can be obtained simply by "crossing" the result for $e^-\mu^- \to e^-\mu^-$, which amounts to the interchange $s \leftrightarrow t$ in Eq. 5.22. Thus,

$$\sum_{\text{spins}} |\mathcal{M}_{fi}|^2 \approx 2e^4 \frac{(t^2 + u^2)}{s^2}, \tag{5.23}$$

where now $e^+e^- \to \mu^+\mu^-$ is the s-channel process.

We can calculate s, t, and u in terms of the center-of-mass energy E_{CM} and the scattering angle θ between the outgoing muons and the incoming electrons (*Exercise: derive these relations.*)

$$\begin{aligned} s &= E_{\text{CM}}^2, \\ t &= \frac{1}{2}E_{\text{CM}}^2(1 - \cos\theta), \\ u &= \frac{1}{2}E_{\text{CM}}^2(1 + \cos\theta). \end{aligned} \tag{5.24}$$

Therefore,

$$\sum_{\text{spins}} |\mathcal{M}_{fi}|^2 \approx e^4(1 + \cos^2\theta), \tag{5.25}$$

and the differential cross section is

$$\frac{d\sigma}{d\Omega}_{\text{CM}} = \frac{2e^4}{64\pi^2 s}\left(\frac{1}{2}(1 + \cos^2\theta)\right) = \frac{\alpha^2}{4s}(1 + \cos^2\theta), \tag{5.26}$$

where we have made the substitution $\alpha = \dfrac{e^2}{4\pi}$. Note that, unlike $e^-\mu^- \to e^-\mu^-$, this cross section shows only a mild peaking in the forward direction.

The total interaction cross section can be obtained by integrating over θ:

$$\sigma(e^+e^- \to \mu^+\mu^-) = \frac{4\pi\alpha^2}{3s}. \tag{5.27}$$

It falls as the inverse-square of the CM energy.

This result has been verified by experimental data at E_{CM}'s up to several tens of GeV, until effects of weak interaction become significant. Up to that point, the error incurred by ignoring higher order terms in the perturbative calculations (corresponding Feynman diagrams have multiple iternal lines) is much smaller than the experimental resolution.